

# The Predicted Coiled-coil Domain of Myosin 10 Forms a Novel Elongated Domain That Lengthens the Head\*

Received for publication, May 3, 2005, and in revised form, June 24, 2005 Published, JBC Papers in Press, July 18, 2005, DOI 10.1074/jbc.M504887200

Peter J. Knight<sup>‡§</sup>, Kavitha Thirumurugan<sup>‡§</sup>, Yuhui Xu<sup>¶</sup>, Fei Wang<sup>¶</sup>, Arnout P. Kalverda<sup>||</sup>, Walter F. Stafford III<sup>\*\*</sup>, James R. Sellers<sup>¶</sup>, and Michelle Peckham<sup>‡1</sup>

From the <sup>‡</sup>School of Biomedical Sciences, <sup>§</sup>Astbury Centre for Structural Molecular Biology, and <sup>||</sup>School of Biochemistry and Microbiology, University of Leeds, Leeds, LS2 9JT, United Kingdom, <sup>\*\*</sup>Boston Biomedical Research Institute, Analytical Ultracentrifugation Research Laboratory, Boston, Massachusetts 02472-2829, and <sup>¶</sup>Laboratory of Molecular Physiology, NHLBI, National Institutes of Health, Bethesda, Maryland 20892-1762

Myosin 10 contains a region of predicted coiled coil 120 residues long. However, the highly charged nature and pattern of charges in the proximal 36 residues appear incompatible with coiled-coil formation. Circular dichroism, NMR, and analytical ultracentrifugation show that a synthesized peptide containing this region forms a stable single  $\alpha$ -helix (SAH) domain in solution and does not dimerize to form a coiled coil even at millimolar concentrations. Additionally, electron microscopy of a recombinant myosin 10 containing the motor, the three calmodulin binding domains, and the full-length predicted coiled coil showed that it was mostly monomeric at physiological protein concentration. In dimers the molecules were joined only at their extreme distal ends, and no coiled-coil tail was visible. Furthermore, the neck lengths of both monomers and dimers were much longer than expected from the number of calmodulin binding domains. In contrast, micrographs of myosin 5 heavy meromyosin obtained under the same conditions clearly showed a coiled-coil tail, and the necks were the predicted length. Thus the predicted coiled coil of myosin 10 forms a novel elongated structure in which the proximal region is a SAH domain and the distal region is a SAH domain (or has an unknown extended structure) that dimerizes only at its end. Sequence comparisons show that similar structures may exist in the predicted coiled-coil domains of myosins 6 and 7a and MyoM and could function to increase the size of the working stroke.

Myosins make up a diverse superfamily of motor proteins (1). The human genome alone contains about 40 myosin genes (2). Of these, about one-third are “conventional” myosins (*i.e.* the well studied myosin 2), and the rest fall into about 10 different classes. The structure, properties and functions of the majority of myosin classes are poorly characterized and have largely been inferred from sequence comparisons rather than direct experiments on purified proteins (1–3).

Muscle myosin 2 dimerizes through its  $\alpha$ -helical coiled-coil tail. Therefore, it is commonly assumed that any myosin will also be dimeric if it contains a region predicted to be coiled coil. This assumption is dependent on the accuracy of coiled-coil prediction programs, such as COILS (4), PAIRCOIL, or MULTICOIL (5), which are also used by protein-fold prediction sites on the Web such as SMART (6).

Although myosin 10 contains a region of predicted coiled coil (Fig. 1A), and is predicted to dimerize, this has not been determined experimentally. We noticed that part of the predicted coiled-coil domain of myosin 10 is highly enriched in charged residues (Fig. 1B). The proximal region consisting of 36 residues is particularly enriched in both positively and negatively charged residues, including the *a* and *d* positions of the heptad repeat (*a*–*g*) that are canonically hydrophobic residues in coiled coils (Fig. 1B). We suspected that this highly charged sequence is unlikely to form a coiled coil (7), suggesting that this part of myosin 10 may not be able to dimerize.

To determine the properties of the predicted coiled-coil domain of myosin 10, we studied a purified synthetic peptide containing the proximal highly charged region to determine its structure in solution. We then went on to determine the structure of the full-length predicted coiled coil of myosin 10 by electron microscopy, using a recombinant expressed myosin 10 containing the motor, calmodulin binding domains, and full-length predicted coiled coil.

## MATERIALS AND METHODS

**Peptide Purification**—The peptide YRQLLAEKRELEEKRRREEEKK-REEERERERAQREC, which corresponds to residues 808–843 of murine myosin 10 with an additional C-terminal Cys, calculated mass 4,876.5 Da, was made commercially (Pepceuticals) and further purified using reverse phase high pressure liquid chromatography (University of Leeds). Major peaks that were likely to contain the peptide were analyzed by matrix-assisted laser desorption ionization-mass spectrometry to identify the correct peak. Fractions containing the purified peptide in 30% acetonitrile/70% H<sub>2</sub>O/0.1% trifluoroacetic acid were combined and freeze dried.

**Circular Dichroism**—Spectra were recorded using a Jasco J715 from 260 to 190 nm at 10 °C in a 1-mm cuvette at 46  $\mu$ M peptide (0.2 mg/ml) in 100 mM NaF, 10 mM sodium phosphate, pH 7.0. Spectra were also recorded from a solution of rabbit skeletal muscle myosin subfragment 2 (S2)<sup>2</sup> at the same mass concentration and in the same buffer. To determine the effect of temperature on helical content, we took measurements at a wavelength of 222 nm during a series of temperature steps to 80 °C for the peptide and S2, after which the temperature was returned to 10 °C to observe refolding. The peptide was allowed to equilibrate at each temperature until the average ellipticity measurement from a 1-min scan remained constant between observations. To determine the effect of peptide concentration, we compared data from solutions containing 225 or 22.5  $\mu$ M peptide dissolved in 10 mM MOPS, pH 7.0, at 10, 25, 50, and 70 °C. The effect of salt concentration on helical

\* This work was supported by the Wellcome Trust and the Biotechnology and Biological Sciences Research Council (United Kingdom). The costs of publication of this article were defrayed in part by the payment of page charges. This article must therefore be hereby marked “advertisement” in accordance with 18 U.S.C. Section 1734 solely to indicate this fact.

<sup>1</sup> To whom correspondence should be addressed: School of Biomedical Sciences, Worsley Bldg., University of Leeds, Leeds LS2 9JT, United Kingdom. Tel.: 44-113-343-4348; Fax: 44-113-343-4228; E-mail: m.peckham@leeds.ac.uk.

<sup>2</sup> The abbreviations used are: S2, subfragment 2; SAH, single  $\alpha$ -helix; HMM, heavy meromyosin; MOPS, 4-morpholinepropanesulfonic acid.

content was determined from the value at 25 °C of the ellipticity measurement at a wavelength of 222 nm for the peptide in 10 mM MOPS, pH 7.0, and a range of NaCl concentrations from 0 to 4.5 M. Spectra were analyzed using the CDSSTR program, available on DICHROWEB (8), and reference set 4 in order to calculate the mean residue ellipticity in degrees  $\text{cm}^2 \text{dmol}^{-1}$  and therefore calculate the fraction of  $\alpha$ -helix. The fittings to the data were good, with normalized root mean square deviations of 0.033–0.037 for the peptide at 10 °C. The actual concentration of the peptide used was determined spectrophotometrically at the end of the experiments using an absorption coefficient of  $1,690 \text{ M}^{-1} \text{ cm}^{-1}$  at 275 nm arising from the N-terminal Tyr and correcting for light scatter using data between 310 and 400 nm. The ellipticity value at 222 nm for myosin 10 peptide in 100 mM NaF, 10 mM sodium phosphate at 10 °C was  $-26,300^\circ \text{ cm}^2 \text{dmol}^{-1}$ .

**Analytical Ultracentrifugation**—Equilibrium runs were performed using 12-mm path length cells in a Beckman Optima XL I at 60,000 rpm, 10 °C for 72 h. The peptide was dissolved in 100 mM NaF, 10 mM sodium phosphate, pH 7.0. Data were gathered by radial scanning at 275 nm (the absorption peak of the peptide). WinMatch was used to determine that the solution column had reached equilibrium. Nominal loading concentrations covered 0.1 to 1 mg/ml. A value for the partial specific volume of 0.719 cc/g was computed from the amino acid composition using the method of Perkins (9). Fitting was performed using the equilibrium fitter now part of SedAnal (10), and error bars were obtained using bootstrap with replacement.

**Proton NMR**—The sample contained 1 mM peptide in 100 mM NaF, 10 mM sodium phosphate, pH 7.0. Data were recorded at 10 °C on 500- and 750-MHz Varian Inova NMR spectrometers equipped with a z-axis gradient triple resonance probe. A 500-MHz 90-ms Watergate TOCSY and 200-ms Watergate NOESY experiment was recorded with  $1024 \times 256$  complex points, spectral windows of 5006.3 Hz, and 64 transients/increment. A 750-MHz 150-ms Watergate NOESY was recorded with  $2,048 \times 512$  complex points, spectral windows of 8,000 Hz, and 48 transients/increment. Spectra were processed with NMRPipe using 30° shifted cosine window functions in both dimensions and analyzed in NMRView. Chemical shifts were referenced to internal 2,2-dimethyl-2-silapentanesulfonic acid. Deviations from random coil chemical shifts were calculated with corrections for the sequence (11, 12).

**Protein Preparations**—Myosin 10 “HMM” was expressed using the baculovirus system. Bovine smooth muscle myosin 10 cDNA clones were a gift from Dr. David Corey (Harvard Medical School). Sequences encoding the first 953 amino acids including the motor domain, the three IQ motifs, and all of the predicted coiled-coil-forming residues (120 residues; the predicted coiled-coil domain ends at amino acid 934) were ligated into pVL1932 (Invitrogen) between the BglII and the XbaI sites. A FLAG epitope was engineered before the stop codon to facilitate purification. Mouse myosin 5a HMM heavy chain (ID NM\_010864; residues 1–1090 plus FLAG sequence), and a mutant lacking IQ motifs 3 and 4 (called M5-4IQ) were expressed together with calmodulin and purified as described by Sakamoto *et al.* (13).

**Electron Microscopy**—For metal shadowing, proteins at about 0.1 mg/ml in 0.5 M NaCl were diluted  $1 \times$  with glycerol as described previously (14), sprayed onto mica, dried under vacuum at room temperature, and rotary-shadowed with platinum. Fields of molecules were recorded on film at  $\times 20,000$  magnification and scanned into computer at a specimen resolution of 1 nm/pixel. For negative staining, myosin 10 HMM was diluted to 56 nM protein with 50 mM KCl, 0.1 mM EGTA, 3 mM  $\text{MgCl}_2$ , and 10 mM MOPS, pH 7.0, at 20 °C, applied to UV-treated carbon-coated grids, and negatively stained with 1% uranyl acetate as described previously (15). Micrographs were recorded at  $\times 40,000$  on a

JEOL 1200ex microscope at moderate dose ( $\sim 100 \text{ e}/\text{\AA}^2$ ) and digitized at a step size corresponding to 0.5 nm/pixel. The head length was measured as the linear distance from one end of the molecule to the other for monomers or up to the junction point of the two heads for dimers.

**Model Building**—The highly charged region of the predicted coiled coil of myosin 10 (37-amino acid peptide) was modeled as an  $\alpha$ -helix with energy minimization of side chain conformation *in vacuo* using a Swiss-Pdb Viewer. This model was then combined with a model structure of a 32-residue IQ motif plus calmodulin (16). Using the Swiss-Pdb Viewer, we superimposed the backbone atoms of the first 12 N-terminal residues of the myosin peptide on those of the homologous residues of the IQ motif. The peptide was then ligated to the IQ motif after removing overlapping residues.

## RESULTS

We suspected that the proximal 36 residues of the predicted coiled coil of myosin 10 formed a single  $\alpha$ -helix (a SAH domain). Displaying these residues as an  $\alpha$ -helical net shows a large number of potential intrahelical ionic interactions that would stabilize formation of a single  $\alpha$ -helix (Fig. 1C). An atomic  $\alpha$ -helical model of this sequence (Fig. 1D) further demonstrates that the alternately positive and negative charged side chains found in this sequence in successive turns of the helix line up to form three left-handed helices by alternate ( $i, i+3$ ) and ( $i, i+4$ ) interactions (Fig. 1, C (solid lines) and D).

SAH domains are rare but have been described for a small number of proteins including smooth muscle caldesmon (17) and the ribosomal protein L9 (18). The heptad repeat in the predicted SAH domain in myosin 10 has the novel general form  $((R/K)XXXEXX)_n$ . The interaction between the distributed positive charge of the guanidinium group of Arg and the distributed negative charge of the carboxylic group of Glu are particularly favorable for helix stabilization (Fig. 1D, space-filled).

**The Highly Charged Sequence Forms a Very Stable SAH Domain in Solution**—To test these ideas, a peptide was synthesized consisting of the first 36 residues of the predicted coiled coil of myosin 10. Its ability to form a SAH domain in solution was measured by a combination of three different techniques.

First, UV circular dichroism (Fig. 2A) showed that this peptide is largely  $\alpha$ -helical, as shown by the strong double minima at 208 and 222 nm, and a stronger maximum at 191–193 nm. Fitting of the spectrum using CDSSTR (DICHROWEB (8)) showed that the peptide is  $\sim 75\%$   $\alpha$ -helical at 10 °C, the remainder being assigned between  $\beta$ -strands and unstructured conformations. These values did not change as the peptide concentration varied between 22.5 and 225  $\mu\text{M}$ , indicating that the peptide is monomeric (19, 20).

We also found that the thermal and salt stability of this peptide is similar to that described for other single stable  $\alpha$ -helices (17–20). Heating to 80 °C reduced the helical content in a non-cooperative manner (Fig. 2B), and this effect was completely reversed on cooling to 10 °C (Fig. 2A). This temperature dependence was markedly different from the cooperative melting of the monomeric S2 region of the coiled-coil tail of muscle myosin 2 (Fig. 2B). The helical content of the peptide falls progressively with increasing salt concentration (Fig. 2C). This is thought to be due to competition from ions in solution with the intrahelical ionic bonds that stabilize single  $\alpha$ -helices. The helical nature of the myosin 10 peptide is even more resistant to salt than the single  $\alpha$ -helix formed by the  $\text{E}_4\text{K}_4$  peptide (amino acid sequence, YSEEEKKEKKEEKKKK) under similar conditions (19), indicating that the intrahelical ionic bonds are unusually strong.

Second, proton NMR confirmed that the peptide is highly helical and that only the first few N-terminal residues are non-helical. The data

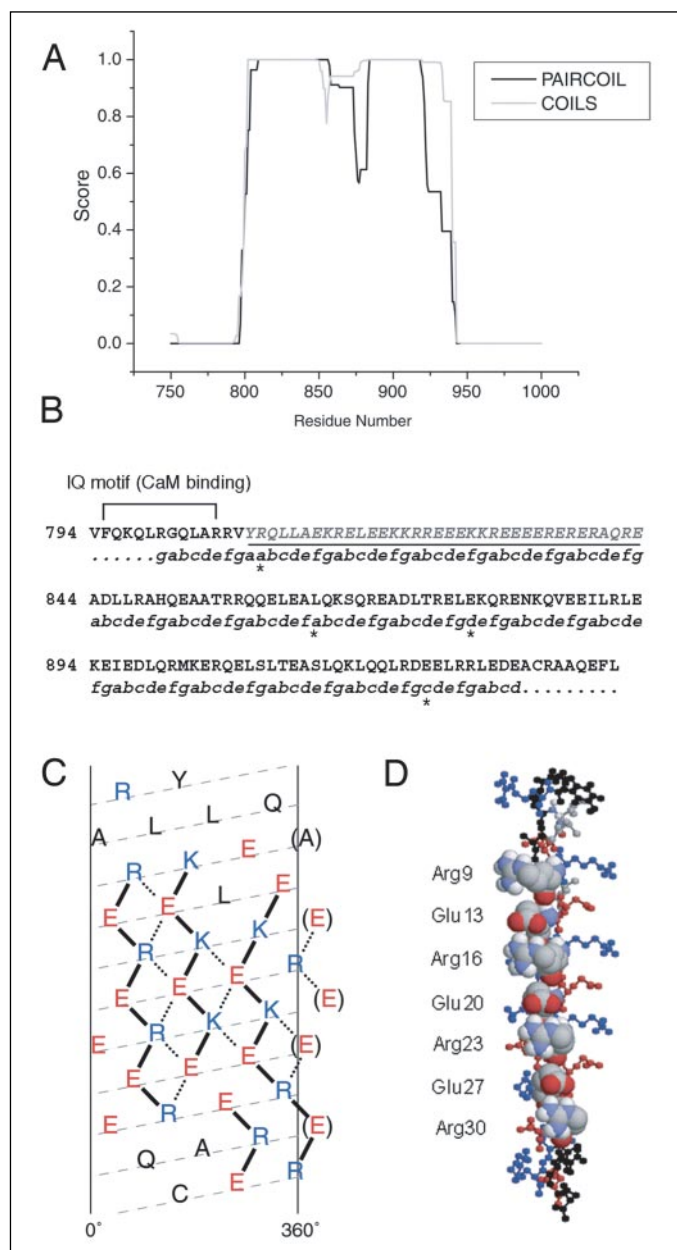


**FIGURE 1. Analysis of the predicted coiled-coil domain of myosin 10.** *A*, PAIRCOIL and COILS scores (using  $a$  and  $d$  weighting of 2.5 and a window of 28 residues) for mouse myosin 10 tail sequence, showing the region predicted to be coiled coil. *B*, the sequence of the region of predicted coiled coil for myosin 10 showing its proximity to the last IQ motif. The highly charged proximal region of the predicted coiled coil is shown in *gray italic font and underlined*. The heptad repeat positions ( $a$ – $g$ ) predicted by the PAIRCOIL program are shown *below* the amino acid sequence if the score exceeds 0.5. The asterisks highlight discontinuities in the assignment for the heptad pattern. *CaM*, calmodulin. *C*, helical net representation of the myosin 10 peptide; helix axis vertical;  $\alpha$ -helix track as dashed gray line; N terminus at top; blue, positive charged side chains; red, negative ones; black, others. For ease of comparison with *D*, the helix net is displayed as if viewed from outside. Dotted lines and solid lines show possible ionic interactions. Residues near left edge of net are duplicated at ( $\phi + 360^\circ$ ) so that all interactions can be drawn. *D*, model of the peptide as an  $\alpha$ -helix, showing the (RXXEXX)<sub>3</sub>R motif as space-filled with Corey-Pauling-Koltun color scheme and sequence position in the peptide shown to the left. Other charged residues are shown as blue (R, K) or red (E).

show that the N-terminal 6 residues are random coil or extended, and the remainder of the peptide, beginning at around residue 7, forms  $\alpha$ -helix. From an analysis of the 750-MHz NOESY spectrum (proton NMR) assignments could be obtained for the N-terminal residues 3–7 and the C-terminal residues 30–37 (Fig. 3, *A* and *B*). The N-terminal residues show weak amide-amide and strong NH-H $\alpha_{(i-1)}$  nuclear Over-

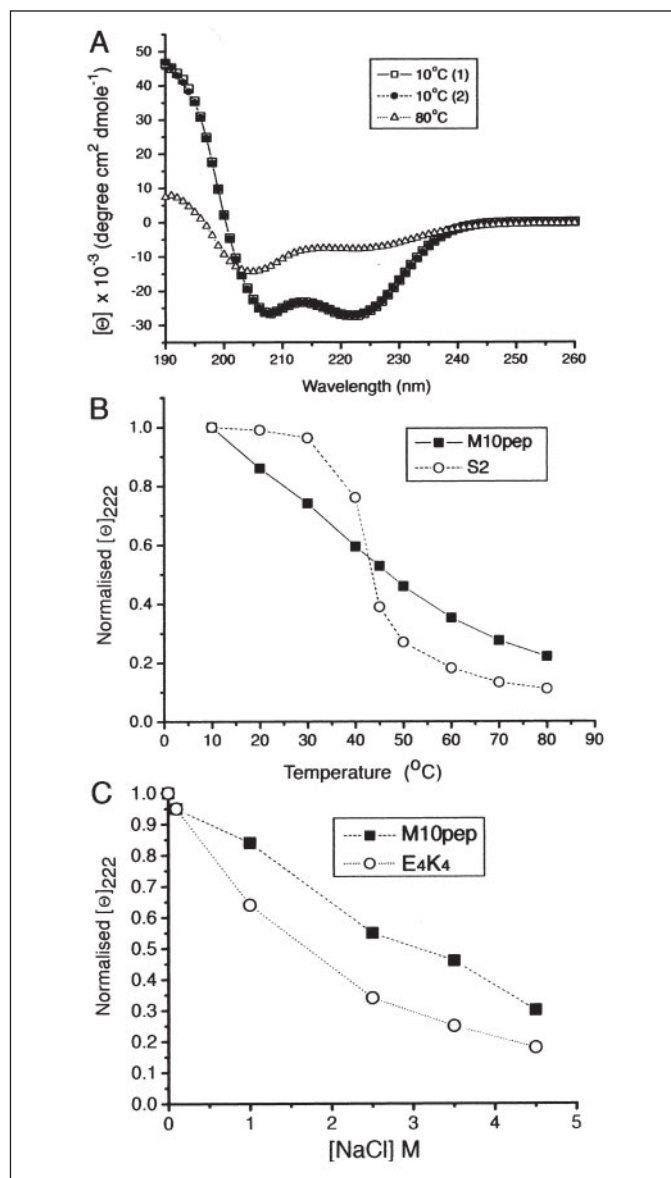


**FIGURE 2. Characteristics of the myosin 10 peptide by UV circular dichroism.** *A*, spectra of the myosin 10 peptide at 10  $^\circ\text{C}$  (before and after heating to 80  $^\circ\text{C}$ ; data essentially superimpose) and 80  $^\circ\text{C}$ . *B*, mean residue ellipticity at 222 nm as a function of temperature. Samples were made in 100 mM NaF, 10 mM sodium phosphate, pH 7.0. Peptide concentration was 46  $\mu\text{M}$ . The ellipticity is normalized to the value measured at 10  $^\circ\text{C}$ . For comparison, results for myosin S2 are also shown. *M10pep*, myosin 10 peptide. *C*, mean residue ellipticity at 222 nm as a function of NaCl concentration. Peptide concentration was 22.5  $\mu\text{M}$ . The ellipticity is normalized to the value measured at 25  $^\circ\text{C}$  for the myosin 10 peptide. For comparison, published results (19) for the E<sub>4</sub>K<sub>4</sub> peptide (normalized to the value measured at 4  $^\circ\text{C}$ ) are shown.

hauser effects consistent with a more extended or random coil structure (21). The C-terminal residues show strong amide-amide and weak NH-H $\alpha_{(i-1)}$  nuclear Overhauser effects, which is consistent with an  $\alpha$ -helical structure. This is in good agreement with the chemical shift deviations from random coil values (Fig. 3, *C* and *D*) that show significant upfield shifts for both the NH and H $\alpha$  protons in the C-terminal region. The intermediate residues are difficult to assign because of the repetitive pattern of the residues Arg, Lys, and Glu in this region. However, the resonance positions for the middle region of the peptide, although heavily overlapped in the spectra, are also consistently shifted upfield from the random coil chemical shifts, indicating that the Lys-Arg-Glu-rich sequence is most likely  $\alpha$ -helical throughout.

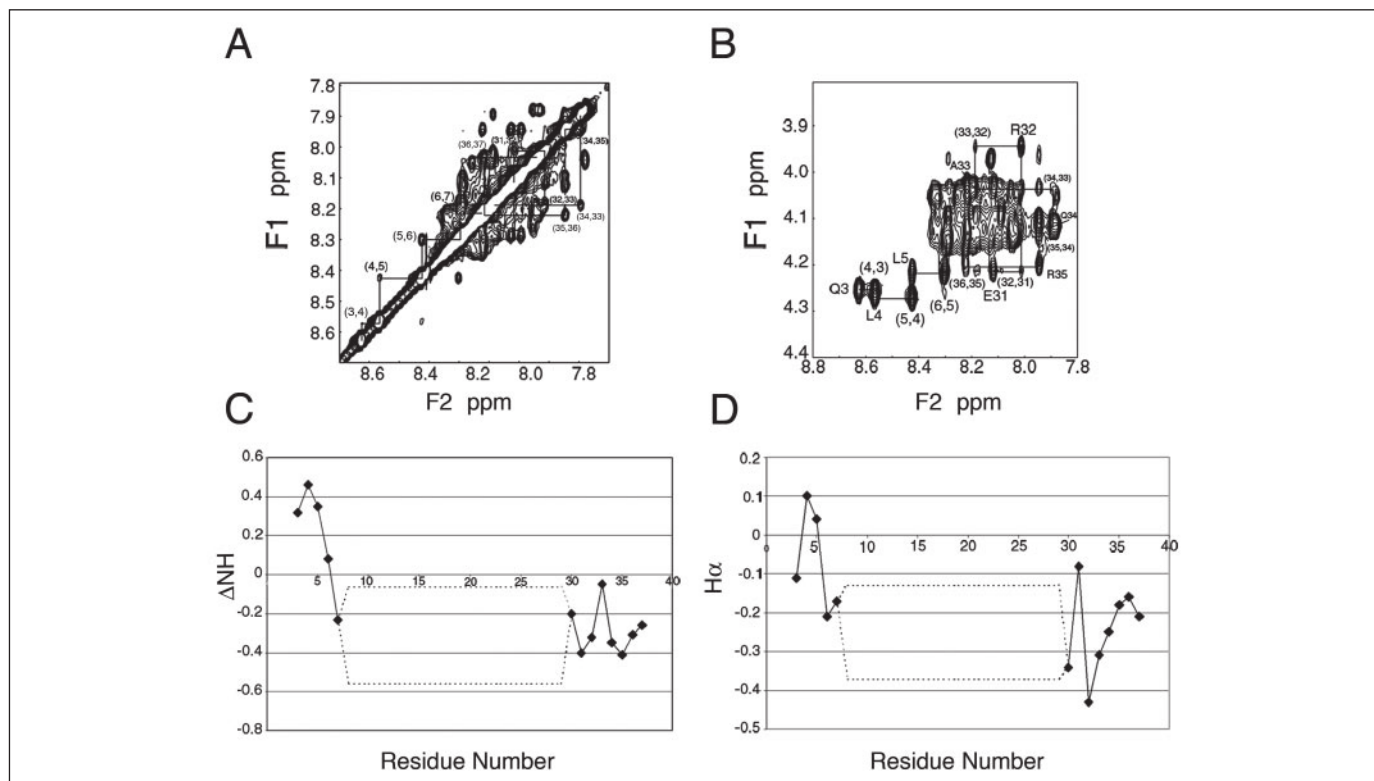


FIGURE 3. Proton NMR analysis of the myosin 10 peptide. *A*, NH-NH region. *B*, NH-H $\alpha$  region, of 150 ms NOESY spectrum at 750 MHz. Sequential nuclear Overhauser effects are labeled with residue numbers and connected by lines. *C* and *D*, chemical shift deviations from predicted random coil values. *C*, NH chemical shift deviations. *D*, H $\alpha$  chemical shift deviations. The dashed lines indicate the minimal and maximal chemical shift deviations for the overlapped KRE-rich region based on a NH shift between 8.34 and 7.94 ppm and a H $\alpha$  shift between 4.01 and 4.16 ppm.

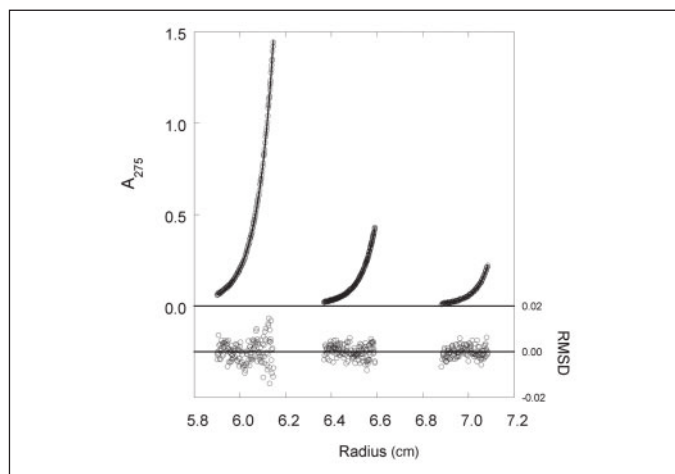


FIGURE 4. Equilibrium analytical ultracentrifugation of the peptide at 60,000 rpm, 10 °C, 100 mM NaF, 10 mM sodium phosphate, pH 7.0, at three loading concentrations (1.0, 0.3, and 0.1 mg/ml). The solid line is the radial distribution of peptide concentration; open circles are points along the fitted line; lower panel shows (observed data – fit) on an expanded scale. RMSD, root mean square deviation(s).

Third, equilibrium analytical ultracentrifugation confirmed that the peptide is monomeric (Fig. 4). The data show that the peptide is monodisperse with a molecular mass of  $4,850 \pm 20$  (S.E.) Da, which agrees closely with the sequence molecular mass of 4,876 Da. These experiments were performed under the same solution conditions as the circular dichroism and NMR. Fitting with SedAnal gave a good fit to the data over a wide range of concentration (Fig. 4). Attempts to fit the data using any fixed ratio of monomer and dimer or a monomer-dimer equilibrium showed there was no detectable dimer over the range of loading

concentrations from 0.1 to 1.0 mg/ml with an upper limit of 3.4 mg/ml (0.7 mM) in the solution column at equilibrium.

Taken together, these data show that the highly charged region of myosin 10 is stable SAH domain as we predicted. The highly helical nature of this peptide suggests that it is unlikely to have failed to dimerize because it was too short. Short sections of coiled coil that do not dimerize also fail to form an  $\alpha$ -helix (22), whereas peptides that have an optimum sequence for formation of coiled coil only need to be 2 heptads long to dimerize (23). Other peptides that are only 4 heptads long and rich in either Lys or Glu residues form stable heterodimers when mixed but random coil monomers when kept separate (22).

*The Entire Predicted Coiled Coil Is Extended and Only Weakly Dimeric*—The next question was whether this region of myosin 10 formed a SAH domain in the intact myosin rather than dimerizing to form a coiled coil. We suspected that the SAH domain would not dimerize via coiled-coil formation, as the SAH domain sequence (Fig. 1*B*) does not have any hydrophobic residues in the *a* and *d* positions that would favor dimerization (24). However, it was possible that in the intact molecule this region could be induced to dimerize through charged interactions following dimerization by the rest of the predicted coiled coil, by analogy with the GCN4 zipper-induced dimerization of a similarly charged region in myosin 6 (25).

To address this question, we used electron microscopy to investigate the structure of the entire coiled-coil domain in a recombinant fragment of myosin 10 that contained the motor, the three calmodulin binding domains, and the full-length (120 residues) predicted coiled coil. The concentrations used in these studies were similar to those *in vivo* (i.e. nanomolar (26)). It is worth noting that we used this recombinant fragment rather than the full-length native myosin 10 because this myosin is not abundant (26) and thus has not been successfully purified

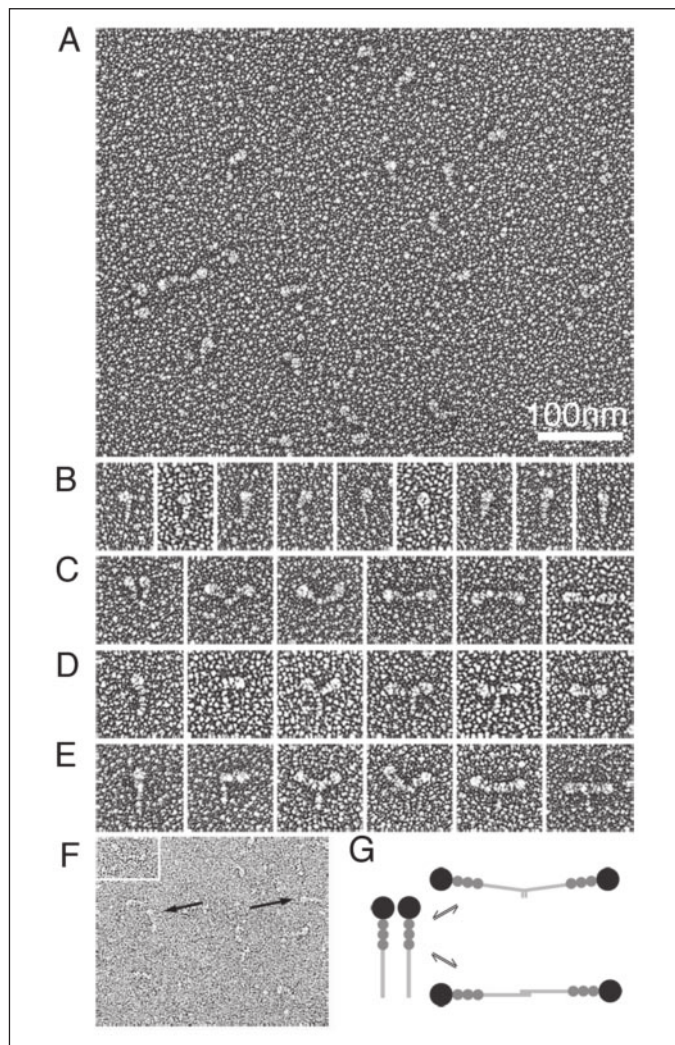


**FIGURE 5. Electron microscopy of recombinant fragments of myosins 10 and 5.** *A*, field of rotary-shadowed recombinant myosin 10 showing mainly single-headed molecules. *B* and *C*, galleries illustrating the range of appearances of single-headed and double-headed molecules of recombinant myosin 10. *D* and *E*, galleries of myosin 5 HMM 4IQ and 6IQ, respectively, from the same rotary shadowing experiment. Two examples of uncommon single-headed molecules are shown on the left; double-headed molecules are shown on right. *F*, field of negatively stained myosin 10 HMM showing single-headed molecules (arrows). A dimer is shown in the inset. *G*, a scale diagram of myosin 10 HMM region showing dimerization of monomers (34 nm long) to form either parallel (top) or antiparallel (bottom) dimers. 100-nm scale bar in *A* applies to all panels except *G*.

from tissue samples. In addition, we did not use recombinant full-length myosin 10 because this protein is highly subject to degradation in the *Sf9* cells, possibly because it contains three PEST sequences in its tail, just after the predicted coiled-coil domain.<sup>3</sup>

Both rotary-shadowed and negative-stained images show that about 90% of the molecules of this myosin 10 construct are monomeric (Fig. 5). The remainder of the molecules were dimers, and this low proportion suggests that there could be a weak equilibrium between monomers and dimers, with a binding constant in the micromolar range. In contrast, the majority of molecules of two different myosin 5 constructs containing the full-length coiled coil of 182 residues were dimers. These specimens of myosin 5 and myosin 10 constructs were prepared for microscopy at the same time under the same conditions. One construct (M5-6IQ) contained six calmodulin binding sites/heavy chain, as found in the wild type myosin 5, and the other (M5-4IQ) contained only four,

<sup>3</sup> J. R. Sellers, unpublished data.

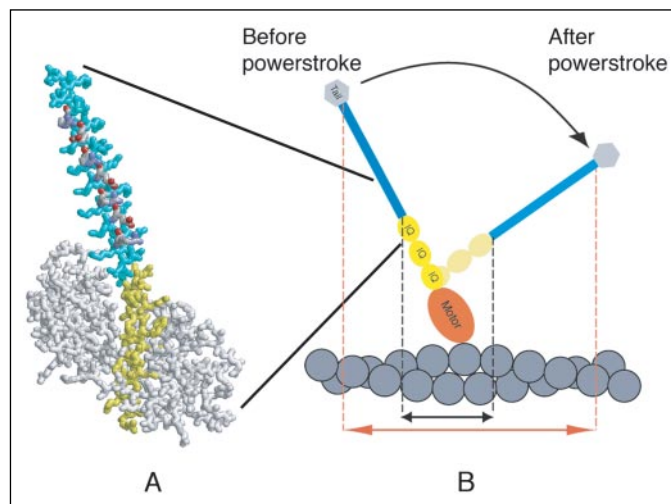


**FIGURE 6. Function of the predicted coiled-coil domain as part of the myosin 10 lever.** *A*, predicted structure of the third IQ region and the SAH domain of myosin 10. The IQ motif is shown in yellow, the peptide (residues 4–37) in cyan, and calmodulin in gray. The (RXXXEXX)<sub>3</sub>R motif of the SAH domain is shown in Corey-Pauling-Koltun colors. *B*, diagram of a monomeric myosin 10 bound to actin, showing the position of the myosin lever before and after the power stroke (as indicated by the curved arrow). The lines linking *A* and *B* show the position of the atomic model within this diagram. If the lever includes the entire predicted coiled-coil domain in an extended form (blue) as suggested by the electron microscopy, the axial component of the working stroke (ignoring the contribution from the motor domain) is increased from the length of the black arrow to that of the red arrow.

which is more directly comparable with myosin 10 (which has three). A few single-headed myosin 5 HMM molecules are seen (Fig. 5, *D* and *E*) that are probably the consequence of the loss of one head by proteolysis in the *Sf9* cells.

A comparison of myosin 5 dimers with those of myosin 10 shows that they have a very different structure (Fig. 5). In myosin 10 dimers, the heads (motor domain and neck) taper toward a narrow neck, and the molecules associate only at the extreme distal ends. The predicted 18-nm coiled-coil tail is not visible, even though many molecules are V-shaped (Fig. 5*C*). This appearance suggests that these molecules could be tethered together by parallel association rather than antiparallel, although we cannot definitely decide between these two alternatives (Fig. 5*G*). We do not know the basis of this dimerization, but if it were due to coiled coil this would be only a few heptads long. In contrast, in myosin 5 the heads do not taper toward a narrow neck and are thicker than the tail, as noted previously for shadowed myosin 2 (27). Furthermore, the short coiled-coil tail of myosin 5 can be easily identified, and its length is close to the 27-nm length expected for the 182 residues predicted to be coiled coil (Fig. 5, *D* and *E*).

Both a simple visual inspection and a measurement of the lengths of the shadowed molecules show that the myosin 10 heads are much longer than expected. The images show that myosin 10 heads are obviously longer than those of M5-4IQ and also longer than those of M5-6IQ, which has twice as many calmodulins per head as myosin 10 (Fig. 5, *D* and *E*). To quantify this observation, we measured the head lengths for myosin 5 and myosin 10 and compared them with the expected head lengths based on the motor domain and number of calmodulins. For myosin 10, the mean head lengths were  $34.7 \pm 4.4$  (S.D.) nm ( $n = 27$ ) and  $32.7 \pm 3.9$  nm ( $n = 28$ ) for monomers and dimers, respectively. These values are much longer than the expected head length of 18.4 nm, based on 8 nm for the motor domain and 10.4 nm for the three calmodulins. For myosin 5, the mean head lengths were  $26.0 \pm 4.2$  nm ( $n = 20$ ) and  $30.9 \pm 4.1$  nm ( $n = 21$ ) for M5-4IQ and M5-6IQ, respectively. These values are close to those expected, 22.4 and 29.6 nm for M5-4IQ

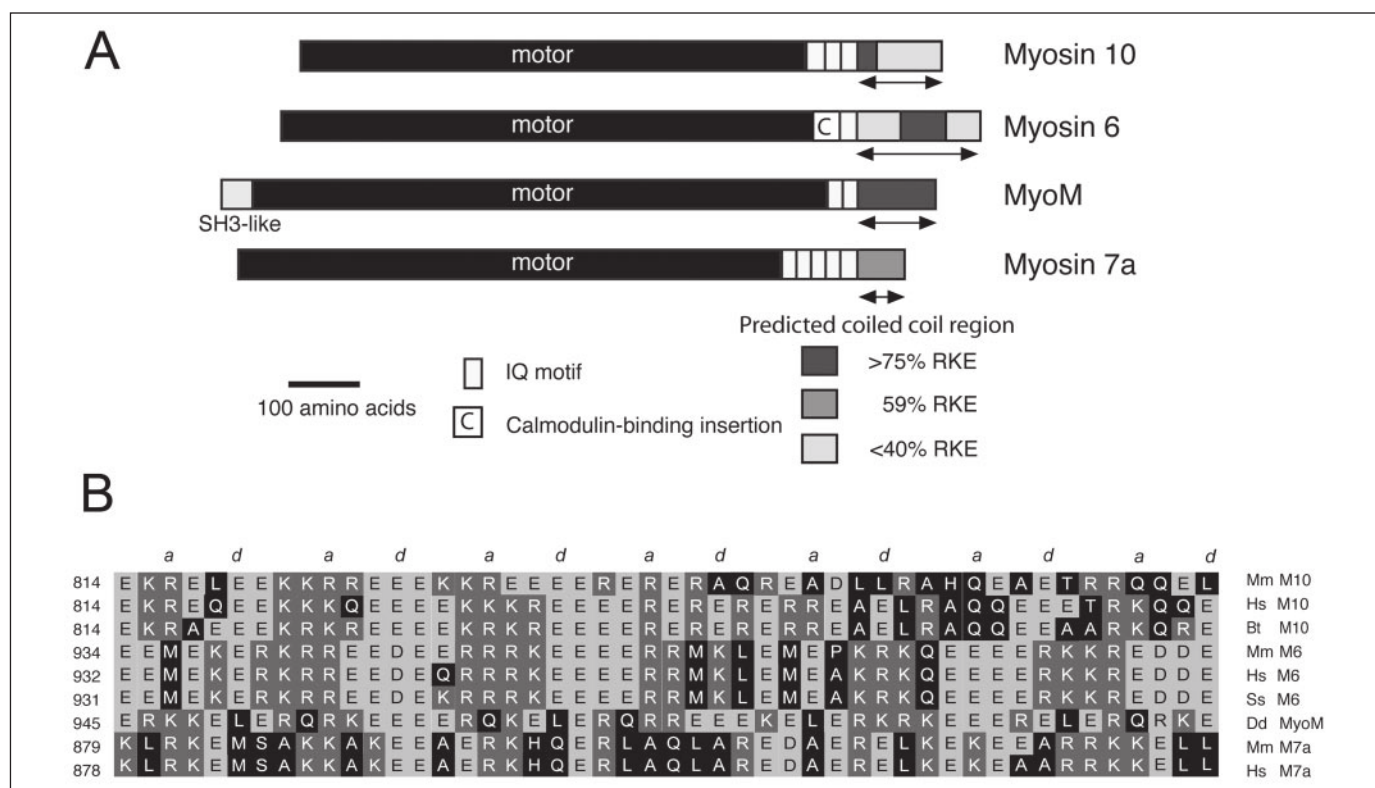


**FIGURE 7. Highly charged regions in the predicted coiled coils of other myosins.** *A*, diagrammatic representation of the motor, IQ, and putative coiled-coil domains of myosins 10, 6, MyoM, and 7a, aligned by the start of the predicted coiled-coil regions. The predicted coiled-coil regions for myosins 10, 6, and MyoM are divided into regions in which either >75% or <40% of the residues are charged (*R*, *K*, or *E* residues) for myosins 10, 6, and MyoM. For myosin 7a the proportion of charged residues was similar throughout (59%). *B*, alignment of 48 residues from part of the putative coiled-coil domains of myosins 10, 6, MyoM, and 7a. The number of the first residue for each sequence is shown to the left. The start of these sequences has been aligned according to the predicted coiled-coil heptad assignments, and the *a* and *d* positions for *Mus musculus* (*Mm*) myosin 10 are shown at the top. Positively charged residues Arg (*R*) and Lys (*K*) are shown in dark gray boxes, negatively charged residues Glu (*E*) and Asp (*D*) in light gray, and all other residues in black. *Bt*, *Bos taurus*; *Dd*, *Dictyostelium discoideum*; *Hs*, *Homo sapiens*; *Ss*, *Sus scrofa*.

and M5-6IQ, respectively. Both metal grain and orientation of the heads can cause a spread in measured values. However, the fact that the myosin 5 data are close to expected values indicates that these effects are minor and that the measured lengths of myosin 10 heads are reliable.

## DISCUSSION

The proximal region of the predicted coiled-coil domain of myosin 10 is highly charged with alternate positively and negatively charged regions, and we predicted that it would form a stable SAH domain rather than a coiled coil. The data presented here confirm this prediction. Our electron microscopy further shows that the majority of the predicted coiled-coil domain does not dimerize to form a tail, but it forms a novel structure that acts to lengthen the head by about 15 nm.

We suspect that the whole of this novel elongated structure is a SAH domain, even though we have so far shown only that the proximal region has this structure, and this is despite the distal region containing hydrophobic residues in *a* and *d* positions that might have been expected to stabilize the coiled coil (Fig. 1*B*). There are two lines of evidence that support this suspicion. First, the heads are longer than can be accounted for by the number of calmodulins and the short SAH domain. Second, the electron microscopy did not show the expected coiled-coil tail. Furthermore, a SAH domain consisting of all 120 residues would be 18 nm long, which is remarkably similar to the ~15-nm difference between measured and expected head lengths. It should be noted that the presence of hydrophobic residues at the *a* and *d* positions (Fig. 1*B*) is not necessarily a good predictor of coiled coil formation, because segments of myosin 2 tails up to about 100 residues long can be monomeric and largely unstructured in solution (28).

The SAH domain is found immediately adjacent to the last IQ motif in the neck of the myosin 10 (Fig. 1*B*), suggesting the intriguing possibility that the SAH domain extends the length of the lever, which is supported by the electron microscopy data. An atomic model of the relationship of the third IQ domain to the SAH domain (Fig. 6*A*), shows that the non-helical N-terminal residues of the myosin 10 peptide can be stabilized in the  $\alpha$ -helical conformation by interaction with the N-terminal lobe of the third calmodulin of the myosin 10 neck in the intact molecule (Fig. 6*A*). Therefore, the SAH domain can be connected directly to the neck without an intervening flexible region and thus can contribute directly to lever action. Our electron microscopy supports this idea, as the long heads of myosin 10 were no more diverse in shape than those of myosin 5 (Fig. 5), suggesting that they are no more flexible.

The length of the lever is important for defining the size of the working stroke of a myosin. The working stroke is the distance that the end of the lever moves through during a cycle of interaction with actin and is a fundamental property of the myosin. According to the current dogma, the number of light chain binding motifs (IQ motifs) in the neck determines the length of the lever. If the proximal 36-residue SAH domain forms part of the lever it would extend its length from 10.4 nm contributed by the three IQ motifs by an extra 5.4 nm, increasing the effective lever length by 50%. If the entire elongated region of ~15 nm contributed to the lever, this would increase the effective lever length by 140% (Fig. 6*B*).

As we had demonstrated the presence of a SAH domain in myosin 10, we wondered whether the predicted coiled-coil domains of other classes of myosin were more likely to be SAH domains instead. Therefore, we looked for the presence of highly charged regions in the predicted

## A Single $\alpha$ -Helix in Myosin 10

coiled-coil domains in other classes. We found that the entire sequences of the predicted coiled coil of myosins 7a and MyoM are highly charged, show a pattern of alternating positive and negative charges that is similar to the pattern found in myosin 10, and are found next to the last IQ motif (Fig. 7). This suggests that these myosins also contain a SAH domain in place of the coiled coil that will extend the lever. For myosin 7a, which has five IQ domains (16.8 nm), the SAH domain (75 residues, 11.7 nm) would increase the effective lever length by 70%. In MyoM, which has two IQ domains (7.8 nm), the predicted SAH domain (~90 residues), would be 14 nm long and therefore would increase the effective lever length by 180%. In addition, we predict that these myosins should be monomeric and not dimeric as proposed originally.

In addition, we found that myosin 6 also contains a highly charged domain in its predicted coiled coil, as noted previously (29). Interestingly, this is also the region with the highest score in coiled-coil prediction programs. However, in this myosin, the highly charged region of the predicted coiled-coil domain is distal rather than proximal to the motor domain as it is separated from the single IQ motif by ~75 residues. It begins at residue 916 and is composed of 67 residues (10 nm of  $\alpha$ -helix). This region has been seen to self-associate when a leucine zipper ties the two chains together (25). However, our data suggest that this is unlikely to happen in the absence of the zipper as the charged nature of this region and the pattern of intrahelical ion pairs is similar to that for myosin 10 (Fig. 7B). We have shown here that the highly charged proximal region of the predicted coiled coil of myosin 10 does not self-associate even at concentrations a million times higher than *in vivo*. In agreement with this, full-length myosin 6 was recently shown to be monomeric (29).

Could the SAH domain contribute to the lever in myosin 6? Myosin 6 has a large working stroke (18 nm) that is difficult to explain on the basis of the classic lever mechanism, as its neck is only 8 nm long (29). A solution to this difficulty has been proposed by combining a large angle of swing of the lever with an extension of the lever beyond the IQ domains into the first part of the putative coiled-coil domain (29). However, if the entire predicted coiled-coil domain (residues 892–1013 in human myosin 6, which have a cut-off score of >0.5 using the COILS prediction program) was a SAH domain, it could extend the lever by 18.2 nm. This could then explain the large working stroke of this myosin without having to invoke a particularly large angle of swing. Furthermore, it could also explain the long strides of the processive myosin 6 HMM construct that is artificially dimerized (30).

In conclusion, our data indicate that myosins 6, 7a, 10, and MyoM contain SAH domains instead of the predicted coiled coil. This raises the possibility that all of these myosins are monomeric and that the SAH domain may lengthen their levers. These are important concepts to test, as monomers will function differently in cells to dimers. For example, native monomeric myosin 6 is not a processive motor (29), whereas forcible dimerization of myosin 6 converts it to a processive motor (30).

It is possible that functional oligomerization in cells by accessory proteins could exploit this property to favor processivity when required. In addition, an increase in the length of the lever will increase the size of the working stroke. It will be important in the future to test whether the predicted SAH domains in other myosins actually adopt that conformation and to establish the contribution they might make to the properties of the lever.

*Acknowledgments*—We thank Drs Jeff Keen and Chris Adams for advice on peptide synthesis and purification, Andy Baron for performing the analytical ultracentrifuge runs, and Prof. Stephen Baldwin for discussions.

## REFERENCES

1. Hodge, T., and Cope, M. J. (2000) *J. Cell Sci.* **113**, 3353–3354
2. Berg, J. S., Powell, B. C., and Cheney, R. E. (2001) *Mol. Biol. Cell* **12**, 780–794
3. Mermall, V., Post, P. L., and Mooseker, M. S. (1998) *Science* **279**, 527–533
4. Lupas, A., Van Dyke, M., and Stock, J. (1991) *Science* **252**, 1162–1164
5. Berger, B., Wilson, D. B., Wolf, E., Tonchev, T., Milla, M., and Kim, P. S. (1995) *Proc. Natl. Acad. Sci. U. S. A.* **92**, 8259–8263
6. Letunic, I., Copley, R. R., Schmidt, S., Ciccarelli, F. D., Doerks, T., Schultz, J., Ponting, C. P., and Bork, P. (2004) *Nucleic Acids Res.* **32**, (suppl.) D142–D144
7. Offer, G., and Sessions, R. (1995) *J. Mol. Biol.* **249**, 967–987
8. Lobley, A., Whitmore, L., and Wallace, B. A. (2002) *Bioinformatics (Oxf)* **18**, 211–212
9. Perkins, S. J. (1986) *Eur. J. Biochem.* **157**, 169–180
10. Stafford, W. F., and Sherwood, P. J. (2004) *Biophys. Chem.* **108**, 231–243
11. Schwarzwinger, S., Kroon, G. J., Foss, T. R., Chung, J., Wright, P. E., and Dyson, H. J. (2001) *J. Am. Chem. Soc.* **123**, 2970–2978
12. Wishart, D. S., Sykes, B. D., and Richards, F. M. (1991) *J. Mol. Biol.* **222**, 311–333
13. Sakamoto, T., Wang, F., Schmitz, S., Xu, Y., Xu, Q., Molloy, J. E., Veigel, C., and Sellers, J. R. (2003) *J. Biol. Chem.* **278**, 29201–29207
14. Wang, F., Chen, L., Arcucci, O., Harvey, E. V., Bowers, B., Xu, Y., Hammer, J. A., III, and Sellers, J. R. (2000) *J. Biol. Chem.* **275**, 4329–4335
15. Burgess, S. A., Walker, M. L., Thirumurugan, K., Trinick, J., and Knight, P. J. (2004) *J. Struct. Biol.* **147**, 247–258
16. Houdusse, A., Silver, M., and Cohen, C. (1996) *Structure (Lond.)* **4**, 1475–1490
17. Wang, E., and Wang, C.-L. A. (1996) *Arch. Biochem. Biophys.* **329**, 156–162
18. Kuhlman, B., Yang, H., Bolce, J., Fairman, R., and Raleigh, D. (1997) *J. Mol. Biol.* **270**, 640–647
19. Lyu, P. C., Gans, P. J., and Kallenbach, N. R. (1992) *J. Mol. Biol.* **223**, 343–350
20. Marqusee, S., and Baldwin, R. L. (1987) *Proc. Natl. Acad. Sci. U. S. A.* **84**, 8898–8902
21. Wuthrich, K. (1986) *NMR of Proteins and Nucleic Acids*, pp. 162–175, Wiley, New York
22. Litowski, J. R., and Hodges, R. S. (2001) *J. Pept. Res.* **58**, 477–492
23. Burkhard, P., Ivaninskii, S., and Lustig, A. (2002) *J. Mol. Biol.* **318**, 901–910
24. Kammerer, R. A., Schulthess, T., Landwehr, R., Lustig, A., Engel, J., Aebi, U., and Steinmetz, M. O. (1998) *Proc. Natl. Acad. Sci. U. S. A.* **95**, 13419–13424
25. Rock, R. S., Ramamurthy, B., Dunn, A. R., Beccafico, S., Rami, B. R., Morris, C., Spink, B. J., Franzini-Armstrong, C., Spudich, J. A., and Sweeney, H. L. (2005) *Mol. Cell* **17**, 603–609
26. Berg, J. S., Derfler, B. H., Pennisi, C. M., Corey, D. P., and Cheney, R. E. (2000) *J. Cell Sci.* **113**, 3439–3451
27. Elliott, A., and Offer, G. (1978) *J. Mol. Biol.* **123**, 505–519
28. Turbedsky, K., and Pollard, T. D. (2005) *J. Mol. Biol.* **345**, 351–361
29. Lister, I., Schmitz, S., Walker, M., Trinick, J., Buss, F., Veigel, C., and Kendrick-Jones, J. (2004) *EMBO J.* **23**, 1729–1738
30. Rock, R. S., Rice, S. E., Wells, A. L., Purcell, T. J., Spudich, J. A., and Sweeney, H. L. (2001) *Proc. Natl. Acad. Sci. U. S. A.* **98**, 13655–13659